Pattern Formation in Crystals

DOI: 10.1002/anie.200601038

Formation of Self-Organized Dynamic Structure Patterns of Barium Carbonate Crystals in Polymer-Controlled Crystallization**

Tongxin Wang, An-Wu Xu, and Helmut Cölfen**

The self-assembly of structural motifs and the self-organization of dynamic motifs into highly ordered one-, two-, or three-dimensional patterns with controlled structures have received much attention in recent years, because of their importance in basic research and their potential applications.[1] Recently, methods such as lithography, microstamping, or template-assisted synthesis have been employed to fabricate patterns with controlled structures.[2] Of the many challenges facing materials science, the development of bottom-up crystallization strategies enabling the direct growth of nanocrystal assemblies with patterns remains an attractive, but elusive goal.

Living organisms accurately and routinely create complex, spatially well-defined functional mesoscopic superstructures, which can now be partly mimicked.[3] Specific additives, such as polymers, can exert a strong influence on crystal nucleation, growth, and self-organization into hierarchical architectures. A number of studies have already attempted to mimic biomineralization by using synthetic polymers as crystal-growth modifiers and superstructure-directing agents.[4] Recently, self-organized $CaCO_3$ crystals with submicrometer-scale periodicity were grown on a thin matrix of a hydrophobically modified polysaccharide in solution, in the presence of poly(acrylic acid) (PAA).[5] Micropatterning of a surface with single crystals of $CaCO_3$ was achieved by using a template-assisted method.[6] Synthetic approaches to the morphological control of inorganic minerals through polymer-controlled crystallization can produce a variety of inorganic superstructures, such as helical fibers, mesocrystals, complex spherical structures, hollow spheres, spongelike structures, and self-similar structures.[7]

Double hydrophilic block copolymers (DHBCs)[4a] consisting of a hydrophilic block that strongly interacts with inorganic minerals and a non-interacting hydrophilic block have recently been employed for the control of mineral crystallization and have proven to be highly effective, improved variants of the polyelectrolytes or amphiphiles used previously.[8] We reported the preparation of helical fibers of $BaCO_3$ using a racemic phosphonated block copolymer as additive.[9] This study demonstrated that the phosphonated group has a strong influence on the crystallization of $BaCO_3$.

In the present paper, we extend these observations through a systematic variation of pH and polymer concentration. We find experimental evidence that self-organization by reaction–diffusion processes, which govern pattern evolution and selection in many chemical and biological systems,[10] can also be realized in biomimetic mineralization. To our knowledge, this case is the first in which self-assembly and self-organization of the primary nanocrystalline building blocks occur in the same chemical system.

The phosphonated block copolymer **6** was synthesized through radical polymerization initiated by the new macroinitiator **4** (Scheme 1; see Supporting Information). Owing to the high steric demand of its functional side groups, the polymer is expected to be stiff, as suggested by computer modeling.[9] The polymer exhibits a high molar mass of

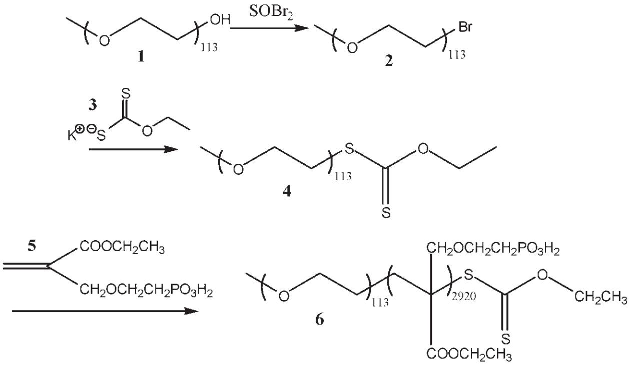

Scheme 1. Synthesis of the phosphonated DHBC **6**.

---

[*] Dr. T. X. Wang,[+] Dr. A.-W. Xu, Dr. H. Cölfen
Max Planck Institute of Colloids and Interfaces
Department of Colloid Chemistry
Research Campus Golm, 14424 Potsdam (Germany)
Fax: (+49) 331-567-9502
E-mail: an-wu.xu@mpikg.mpg.de
coelfen@mpikg.mpg.de

[+] Current address:
Department of Materials Science and Engineering
University of Pennsylvania
3231 Walnut Street, Philadelphia, PA 19104 (USA)

[**] We thank the Max Planck Society for financial support and for a fellowship for T.X.W., and the Alexander von Humboldt Foundation for a research fellowship for A.-W.X. Prof. Markus Antonietti is thanked for the useful discussions. We also thank Antje Völkel for the ultracentrifugation, Ivoclar Vivadent AG (Liechtenstein) for the gift of the acrylate ethyl ester monomer, and Jan Krieger for providing his Brüsselator simulation program free of charge.

Supporting information for this article is available on the WWW under http://www.angewandte.org or from the author.

greater than 700 000 $\mathrm{g\,mol^{-1}}$ and a pH-independent polydispersity in the pH range 1.8–6.5 (see Supporting Information).

Crystallization of $BaCO_3$ through a gas-diffusion procedure (see Supporting Information) in $BaCl_2$ solution (20 mM) with polymer **6** (0.5 $\mathrm{g\,L^{-1}}$) as additive at a starting pH of 3.5 led to ultralong $BaCO_3$ nanofibers, as shown in Figure 1. After 1 day of growth, the resulting $BaCO_3$ crystals consist almost entirely of ultralong nanofibers with diameters of 40–140 nm and lengths of up to several millimeters. Moreover, some nanofibers display a helixlike structure, as observed in our previous study.[9] High-resolution scanning electron microscopy (SEM) images show that each nanofiber is composed of spherical nanoparticles with diameters of approximately 20 nm (Figure 1 b, inset). The spherical nanoparticles self-assemble into the final helical objects. These nanofibers are clearly different from our previous helical fibers, which were assembled from nanorod building blocks.[9] The tectonic assembly of the nanoparticles into a helixlike structure is driven by the selective adsorption of the polymer on a specific crystal face.[9] An X-ray diffraction (XRD) pattern confirms the presence of pure witherite ($BaCO_3$; orthorhombic, space group *Pmcn*, $a=5.316$, $b=8.892$, $c=6.428$ Å (JCPDS 71-2394); see Supporting Information). The primary particle size of 20 nm estimated by SEM agrees well with the XRD data, as evidenced by the reasonable coincidence between the experimental and simulated diffractograms for 20-nm particles of $BaCO_3$. A control experiment in the absence of polymer additive under otherwise similar conditions produced dendritic witherite crystals (see Supporting Information).

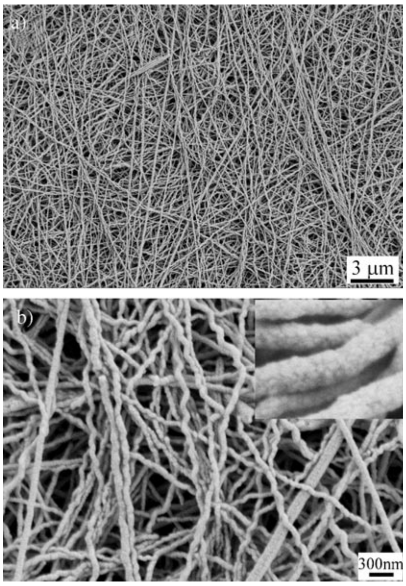

Figure 1. SEM images at different resolutions of ultralong nanofibers of $BaCO_3$ after 1 day of growth ([polymer] = 0.5 $\mathrm{g\,L^{-1}}$, [Ba^{2+}] = 20 mM, starting pH 3.5); inset in (b) is an enlargement.

To investigate their effect on the final product, the polymer (0.5–2 $\mathrm{g\,L^{-1}}$) and Ba^{2+} (2.5–20 mM) concentrations were varied. These experiments indicate that the concentration of polymer, the concentration of Ba^{2+}, and hence, the molar ratio of polymer to Ba^{2+} have a distinct influence on the morphology of the $BaCO_3$ crystals (see Supporting Information). At a fixed Ba^{2+} concentration, a lower polymer concentration favors long nanofibers of $BaCO_3$, implying that the phosphonated block copolymer exerts a strong control on the $BaCO_3$ crystallization. On the other hand, at a fixed polymer concentration, a higher Ba^{2+} concentration favors long nanofibers. At low Ba^{2+} concentrations, short fibers and irregular particles are formed. Our experiments show that a low polymer to Ba^{2+} ratio favors the formation of longer $BaCO_3$ nanofibers. This result might be caused by the strong crystallization-inhibition effect of phosphonated polymers, as shown for $BaSO_4$.[11a] The inhibition is dependent on the polymer concentration, such that the largest number of primary nanoparticles is expected for the lowest polymer and highest Ba^{2+} concentrations. Thus, more and smaller crystallization nuclei are present when CO_2 and NH_3 diffused into the solution.[11b]

In a second set of experiments, the influence of the pH on the morphology of the final products was examined. The solubility of $BaCO_3$ (as well as those of all other carbonates) depends on pH. A lower starting pH means that a larger amount of CO_2 must be added before the precipitation can begin, and therefore, that a higher reactant concentration is present at the point of nucleation. The pH upon dissolution of the polymer in a $BaCl_2$ solution is approximately 3.5. When the starting pH of the solution is 3.5 or 1.8 (adjusted by HCl) and all other conditions are constant, long $BaCO_3$ nanofibers are observed (Figure 2 a,b). Thus, a lower starting pH favors long $BaCO_3$ nanofibers. On the other hand, when the starting pH of the solution is increased to 5.5, rather ill-defined short nanofibers and nanoparticles are observed (Figure 2 c). The higher pH results in earlier nucleation at a lower concentration of reactants, which apparently disturbs the self-assembly into helical fibers. At an even higher pH of 6.5, nucleation leads to spherical $BaCO_3$ aggregates, which coexist with a small number of helical nanofibers (Figure 2 d).

Analytical ultracentrifugation of reaction solutions at different starting pH values confirms that the Ba^{2+} ions form clusters upon hydrolysis at higher pH values, as evidenced by an increase in the sedimentation coefficient (see Supporting

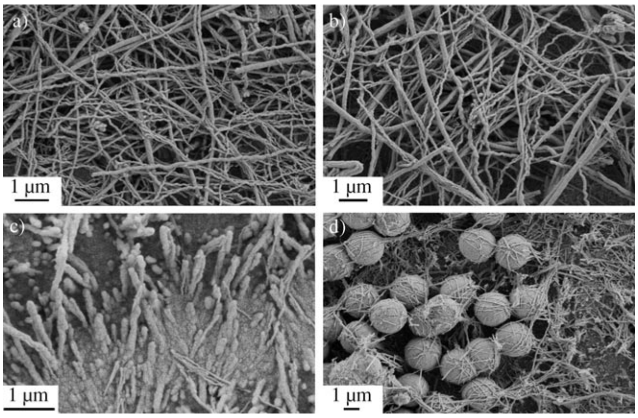

Figure 2. SEM images of $BaCO_3$ crystals after 1 day of growth at starting pH values of a) 1.8, b) 3.5, c) 5.5, and d) 6.5 ([polymer] = 1 $\mathrm{g\,L^{-1}}$, [Ba^{2+}] = 10 mM).

Information). Furthermore, the polymer–Ba^{2+} interaction is pH dependent, and the aggregate size and/or density increases with pH, whereas the polymer itself does not aggregate in the pH range investigated. The polymer–Ba^{2+} aggregation becomes very pronounced at a pH of 6.5, and macroscopic aggregates are formed.

At the critical point between the assembly of $BaCO_3$ into fibers or spheres, the short nanofibers obtained from polymer–Ba^{2+} aggregates at a starting pH of 5.5 self-organize into striking larger-scale structures. Typical SEM images of the quasiperiodic reaction–diffusion patterns observed after 1 day are shown in Figure 3. Light microscopy measurements reveal that these patterns are formed in solution and are not induced by the drying process (see Supporting Information). The periodic wave pattern has multiple centers, from which concentric rings radiate outwards at even spacings (Figure 3 a), and is reminiscent of Liesegang ring patterns[12] or the concentric wave patterns observed in the spatially extended Belousov–Zhabotinsky reaction.[13] On the substrate, many groups of concentric rings grow at the same time and stop before they merge into one another. The distance between adjacent rings is nearly constant at approximately 5 μm (Figure 3), excluding the possibility that these structures are formed by a Liesegang phenomenon. In Liesegang ring patterns, the distance between adjacent rings increases according to $X_n = Q\,(1+p)^n$, where X_n is the position of the nth band, p is the space coefficient (often in the range 0.05–0.4), and Q is a constant. In addition, Liesegang rings are usually formed by imposed concentration gradients in gels, but our ring patterns are formed in dilute solution.

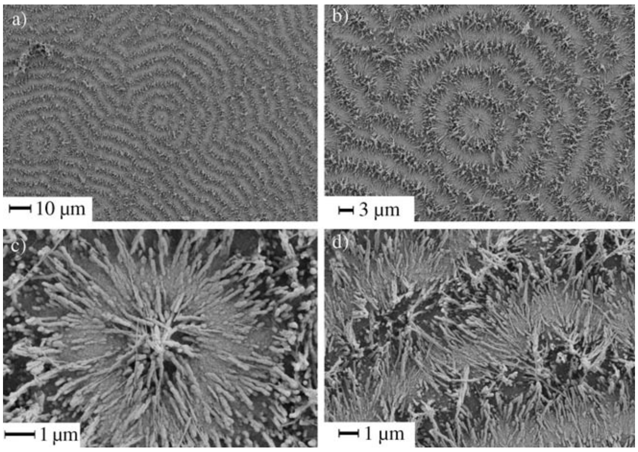

Figure 3. SEM images at different resolutions of the concentric ring patterns of $BaCO_3$ crystals after 1 day of growth ([polymer] = 1 g L^{-1}, [Ba^{2+}] = 10 mM, starting pH 5.5).

The enlarged SEM images show that each ring (band) is composed of short nanorods (Figure 3 c,d). These short nanorods stand, rather than lie, on the substrate and tend to form bundles that are organized in a circular pattern. Note that the experimental window for the formation of this ring pattern is narrow ([polymer] = 0.8–1.3 g L^{-1}, [Ba^{2+}] = 8–12 mM, starting pH 5.1–5.7).

We assume that the periodic pattern formation in the present study belongs to a self-organization process that results from an autocatalytic reaction in counterplay with a diffusion process.[14,15] Such phenomena are usually observed in gel media.[15] To understand the underlying mechanism of the formation of the dynamic ring patterns, we have to formulate the different processes that are equivalent to the elementary steps in a Belousov–Zhabotinsky reaction (see Supporting Information). The Belousov–Zhabotinsky reaction is a self-sustaining reaction–diffusion system;[13] in thin films, straight, spiral, or target oscillating waves of activity propagate as a result. Coupled chemical reactions cause changes in the concentrations of the reagents, which in turn, cause local changes in the oxidation potential of the solution. These potentials can be visualized with a redox indicator.

In our case, the formation of the polymer–Ba^{2+} complex is essential for the oscillating reaction. During complex formation, which is a key step in the autocatalytic cycle, Ba^{2+} ions bind to polymeric polyanions.[16] The formation of the polymer–Ba^{2+} complex can be demonstrated experimentally by titrating a polymer solution with Ba^{2+} and detecting the conductivity (data not shown). Dynamic light scattering measurements indicate that the average size of the polymer–Ba^{2+} complex formed when **6** is added to an aqueous Ba^{2+} solution is approximately 386 nm (data not shown), further confirming the formation of the complex.

Upon subsequent addition of CO_2, $BaCO_3$ is formed primarily in the vicinity of the polymers, which act as localized Ba^{2+} depots. Because of crystallization inhibition at the high local polymer concentration, amorphous nanoparticles of $BaCO_3$ are generated. SEM images of reaction products formed at different growth stages are presented in Figure 4. After 4 h of growth, the product consists of a film composed of particles of approximately 20–30 nm in size (Figure 4 a). The corresponding electron diffraction (ED) pattern confirms that these nanoparticles are amorphous (Figure 4 a, inset).

The amorphous $BaCO_3$ nanoparticles can aggregate. Although the crystallization of an amorphous particle is thermodynamically favored, kinetically inhibition makes it a rare event. If, however, a nanocrystal is formed, the majority of the polymer–Ba^{2+} complex is set free, because at its high local concentration the complex is not included in the crystal lattice, and it is only partially adsorbed onto the nanoparticle surface. The release of the polymer–Ba^{2+} complex upon crystallization is the important autocatalytic step in the observed oscillating reaction. The formation of a nanocrystal, not only results in the crystallization of other amorphous particles in the surrounding aggregate, but also in the attraction of additional amorphous nanoparticles. Similar behavior was also found for crystalline vaterite-type $CaCO_3$ particles formed by the oriented attachment of amorphous precursor particles.[17]

Therefore, the crystalline structure grows quickly and consumes all of the material in its direct surroundings. Consequently, diffusion processes come into play and begin to form the oscillating ring pattern (Figure 4 b). The crystalline nanoparticles aggregate into short fibers, which have a tendency to stand on the substrate (Figure 4 b, inset; similar to ZnO nanorods, which grow vertically on a substrate in solution[18]). The overall precipitation reaction in the presence of the phosphonated polymer **6** can be formulated as

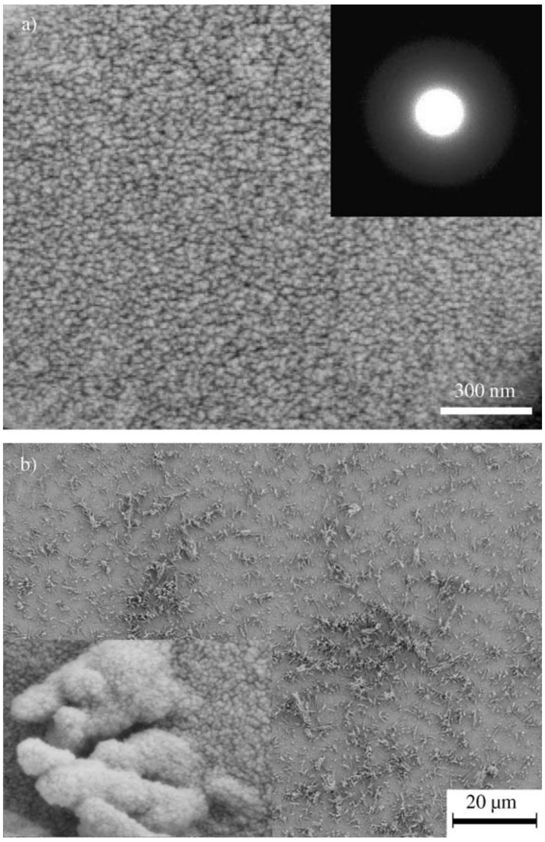

Figure 4. SEM images of the $BaCO_3$ particles after a) 4 h and b) 18 h of growth ($[\text{polymer}]=1\ \mathrm{g\,L^{-1}}$, $[\mathrm{Ba^{2+}}]=10\ \mathrm{mM}$, starting pH 5.5); inset in (a) is the corresponding ED pattern; inset in (b) is an enlargement.

Equation (1) (see Supporting Information for partial reactions).

$$\begin{aligned} & m\,\mathrm{Ba^{2+}} + (m-x)\,\mathrm{H_2O_3P\text{-}polymer\text{-}PO_3H_2} + x\,\mathrm{CO_2} + x\,\mathrm{H_2O} \\ & \rightarrow [\mathrm{BaCO_{3\,cryst}}]_x \downarrow + (m-x)\,[\mathrm{polymer\text{-}(PO_3H)_2Ba}] + 2\,m\,\mathrm{H^+} \end{aligned} \qquad (1)$$

This autocatalytic precipitation reaction coupled with diffusion of the nanoparticles establishes a reaction–diffusion system that leads to a concentric ring pattern. With time, a series of rings propagate out from a common center. To further substantiate that the observed oscillating precipitation reaction is of the Belousov–Zhabotinsky type, we carried out numerical simulations of the reaction–diffusion system using a Brusselator model (see Supporting Information).[19] The simulated pattern evolution in time and space qualitatively agrees with the experimental observations, supporting the oscillating character of our precipitation reaction. Note that similar patterns, although not derived from a Belousov–Zhabotinsky reaction, are also found in biominerals. For example, spiral patterns have been observed on the growing inner surface of nacre (aragonite-type $CaCO_3$); the exact origin of the patterns has not been fully explained.[20]

Many physical, chemical, and biological systems self-organize into periodic patterns characteristic of reaction–diffusion processes.[12–15,21] Examples include periodic precipitation fronts, Liesegang rings, Belousov–Zhabotinsky reactions, chemical turbulence, cardiac waves, and bacterial colonies.

Nature often uses oscillating reactions and similar patterns as a means of producing structures and materials with unique properties that are expressed on scales ranging from macroscopic (for example, stripes in seashells, and annual rings in trees, agates, and rocks) to microscopic (for example, cellular growth, chemotaxis, and biological waves).[21,22] This study adds a new example of spontaneous, self-organized pattern formation in solution by biomimetic mineralization. The resulting patterns are similar to those in a variety of physical, chemical, and natural systems, but are formed by a mesoscale transformation process.

In summary, we report the first Belousov–Zhabotinsky reaction for a self-organized system consisting of nanoparticles. In this system, the coupled reaction partners are not in the same aggregate state (in solution). The relationship between time and space in the observed ring patterns can be elucidated on the basis of the formalism for Belousov–Zhabotinsky oscillating reactions combined with nanoparticle assembly. The formulation of the underlying coupled reactions shows that the autocatalytic step is the formation of a polymer–Ba^{2+} complex. The reaction–diffusion system results in the spontaneous (that is, without external manipulation of concentration, temperature, or any other parameter) formation of micrometer-sized periodic rings of nanocrystalline $BaCO_3$. This ring pattern is grown on a substrate in an aqueous solution containing a new synthetic DHBC. Such a spontaneous generation of a pattern with remarkable regularity on the submicrometer scale is unexpected and indicates that the Belousov–Zhabotinsky reaction may be generalized to systems in different aggregation states (for example, liquid and solid).

The phosphonated block copolymers applied herein interact strongly with inorganic minerals and effectively control the crystallization of $BaCO_3$. A single DHBC can control both crystallization and self-organization by multiple reaction pathways determined by subtle changes in the experimental parameters.

Received: March 15, 2006

Keywords: barium carbonate · Belousov–Zhabotinsky reaction · block copolymers · reaction–diffusion system · self-organization

---

[1] a) A. H. Heuer, D. J. Fink, V. J. Laraia, J. L. Arias, P. D. Calvert, K. Kendall, G. L. Messing, J. Blackwell, P. C. Rieke, D. H. Thompson, A. P. Wheeler, A. Veis, A. I. Caplan, *Science* **1992**, *255*, 1098; b) C. B. Murray, C. R. Kagan, M. G. Bawendi, *Science* **1995**, *270*, 1335; c) G. M. Whitesides, B. Grzybowski, *Science* **2002**, *295*, 2418; d) M. Antonietti, *Nat. Mater.* **2003**, *2*, 9; e) H. Cölfen, S. Mann, *Angew. Chem.* **2003**, *115*, 2452; *Angew. Chem. Int. Ed.* **2003**, *42*, 2350.

[2] a) *Handbook of Microlithography, Micromachining, and Microfabrication* (Ed.: P. R. Choudhury), SPIE, Bellingham, **1997**; b) B. D. Gates, Q. B. Xu, M. Stewart, D. Ryan, C. G. Willson, G. M. Whitesides, *Chem. Rev.* **2005**, *105*, 1171.

[3] a) H. A. Lowenstam, S. Weiner, *On Biomineralization*, Oxford University Press, New York, **1989**; b) S. Mann, *Biomineralization. Principles and Concepts in Bioinorganic Materials Chemis-*

try, Oxford University Press, Oxford, **2001**; c) E. Bäuerlein, *Biomineralization*, Wiley-VCH, Weinheim, **2000**.

[4] a) H. Cölfen, *Macromol. Rapid Commun.* **2001**, *22*, 219; b) F. C. Meldrum, *Int. Mater. Rev.* **2003**, *48*, 187; c) S. H. Yu, H. Cölfen, *J. Mater. Chem.* **2004**, *14*, 2124.

[5] A. Sugawara, T. Ishii, T. Kato, *Angew. Chem.* **2003**, *115*, 5457; *Angew. Chem. Int. Ed.* **2003**, *42*, 5299.

[6] J. Aizenberg, D. A. Muller, J. L. Grazul, D. R. Hamann, *Science* **2003**, *299*, 1205.

[7] a) L. A. Gower, D. A. Tirrell, *J. Cryst. Growth* **1998**, *191*, 153; b) T. Sugawara, Y. Suwa, K. Ohkawa, H. Yamamoto, *Macromol. Rapid Commun.* **2003**, *24*, 847; c) H. Cölfen, M. Antonietti, *Angew. Chem.* **2005**, *117*, 5714; *Angew. Chem. Int. Ed.* **2005**, *44*, 5576; d) S. H. Yu, H. Cölfen, A. W. Xu, W. F. Dong, *Cryst. Growth Des.* **2004**, *4*, 33; e) A. Bigi, E. Boanini, D. Walsh, S. Mann, *Angew. Chem.* **2002**, *114*, 2267; *Angew. Chem. Int. Ed.* **2002**, *41*, 2163; f) L. M. Qi, H. Cölfen, M. Antonietti, M. Li, J. D. Hopwood, A. J. Ashley, S. Mann, *Chem. Eur. J.* **2001**, *7*, 3526.

[8] a) J. M. Marentette, J. Norwig, E. Stockelmann, W. H. Meyer, G. Wegner, *Adv. Mater.* **1997**, *9*, 647; b) M. Antonietti, M. Breulmann, C. G. Göltner, H. Cölfen, K. K. W. Wong, D. Walsh, S. Mann *Chem. Eur. J.* **1998**, *4*, 2493; c) K. L. Robinson, J. V. M. Weaver, S. P. Armes, E. D. Marti, F. C. Meldrum, *J. Mater. Chem.* **2002**, *12*, 890; d) S. H. Yu, H. Cölfen, M. Antonietti, *Chem. Eur. J.* **2002**, *8*, 2937; e) F. Bouyer, C. Gerardin, F. Fajula, J. L. Putaux, T. Chopin, *Colloids Surf. A* **2003**, *217*, 179; f) A. Taubert, D. Palms, O. Weiss, M. T. Piccini, D. N. Batchelder, *Chem. Mater.* **2002**, *14*, 2594.

[9] S. H. Yu, H. Cölfen, K. Tauer, M. Antonietti, *Nat. Mater.* **2005**, *4*, 51.

[10] J. D. Murray, *Mathematical Biology*, Springer, Berlin, **1989**.

[11] a) M. Li, H. Cölfen, S. Mann, *J. Mater. Chem.* **2004**, *14*, 2269; b) T. X. Wang, H. Cölfen, M. Antonietti, *J. Am. Chem. Soc.* **2005**, *127*, 3246.

[12] R. E. Liesegang, *Naturwiss. Wochenschr.* **1896**, *11*, 53.

[13] a) A. N. Zaikin, A. M. Zhabotinsky, *Nature* **1970**, *225*, 535; b) I. R. Epstein, K. Showalter, *J. Phys. Chem.* **1996**, *100*, 13132; c) "Eine periodische Reaktion und ihr Mechanismus": B. P. Belousov in *Selbstorganisation chemischer Strukturen* (Eds.: L. Kuhnert, U. Niedersen), Harry Klein, Frankfurt/Main, **1981**, p. 71.

[14] a) H. K. Henisch, *Periodic Precipitation*, Pergamon, Oxford, **1991**; b) B. Hess, A. Mikhailov, *Science* **1994**, *264*, 223; c) K. Iwamoto, S. Mitomo, M. Seno, *J. Colloid Interface Sci.* **1984**, *102*, 477; d) M. Tsapatsis, D. G. Vlachos, S. Kim, H. Ramanan, G. R. Gavalas, *J. Am. Chem. Soc.* **2000**, *122*, 12864.

[15] a) A. Turing, *Philos. Trans. R. Soc. London Ser. B* **1952**, *237*, 37; b) H.-J. Krug, H. Brandtstädter, *J. Phys. Chem. A* **1999**, *103*, 7811; c) S. C. Müller, J. Ross, *J. Phys. Chem. A* **2003**, *107*, 7997; d) R. Klajn, M. Fialkowski, I. T. Bensemann, A. Bitner, C. J. Campbell, K. Bishop, S. Smoukov, B. A. Grzybowski, *Nat. Mater.* **2004**, *3*, 729.

[16] C. G. Sinn, R. Dimova, M. Antonietti, *Macromolecules* **2004**, *37*, 3444.

[17] N. Gehrke, H. Cölfen, N. Pinna, M. Antonietti, N. Nassif, *Cryst. Growth Des.* **2005**, *5*, 1317.

[18] K. Govender, D. S. Boyle, P. B. Kenway, P. O'Brien, *J. Mater. Chem.* **2004**, *14*, 2575.

[19] a) W. Jahnke, A. T. Winfree, *Int. J. Bifurcation Chaos Appl. Sci. Eng.* **1991**, *1*, 445; b) T. Turänyi, L. Györgyi, R. J. Field, *J. Phys. Chem.* **1993**, *97*, 1931; c) I. Prigogine, R. Lefever, *J. Chem. Phys.* **1968**, *4*, 1695; d) We used the Brusselator simulation program written by Jan Krieger for his "Facharbeit Chemie, Bundeswettbewerb Jugend forscht 2001". This program is based on: J. R. Weimar, *Simulation with Cellular Automata*, Logos, Berlin, **1997**.

[20] K. Wada, *Nature* **1966**, *211*, 1427.

[21] a) M. Tsapatsis, D. G. Vlachos, S. Kim, H. Ramanan, G. R. Gavalas, *J. Am. Chem. Soc.* **2000**, *122*, 12864; b) P. Ortoleva, *Geochemical Self-Organization*, Oxford University Press, Oxford, New York **1994**; c) L. Kuhnert, U. Niedersen, *Selbstorganisation chemischer Strukturen. Ostwalds Klassiker der exakten Wissenschaften*, *Vol. 272*, Geest & Portig, Leipzig, **1987**.

[22] a) P. Ball, *The Self-Made Tapestry: Pattern Formation in Nature*, Oxford University Press, Oxford, **1999**; b) D. Thompson, *On Growth and Form*, Cambridge University Press, Cambridge, **1992**; c) H. Meinhardt, *Models of Biological Pattern Formation*, Academic Press, London, **1982**.